JOURNAL OF PROPULSION AND POWER
Vol. 20, No. 4, July–August 2004

Ammonium Electrolytes Quench Ion Evaporation in Colloidal Propulsion

Rodrigo Bocanegra* and Juan Fernandez de la Mora†
Yale University, New Haven, Connecticut 06520-8286
and
Manuel Gamero-Castaño‡
Busek Company, Inc., Natick, Massachusetts 01760-1023

The desire to improve the specific impulse of colloidal thrusters calls for use of propellants with increasing electrical conductivities, whose electrosprays produce drops of higher and higher charge-to-mass ratio q/m. This favorable trend, however, is limited by the onset of ion evaporation from the tip of the Taylor cone, whereby the combined ejection of ions and drops reduces the propulsion efficiency. This paper studies positively charged electrosprays of formamide seeded with ammonium salts, where the relatively high solvation energy of NH_4^+ eliminates ion evaporation, even at the largest conductivities reached. The effects of solvent and solute volatility are studied by contrasting the behavior of volatile ammonium acetate and involatile ammonium nitrate solutes. The high conductivity and low ionic volatility of the latter lead to record mass-to-charge ratios ($m/q = 0.16$ g/C) and propulsion efficiencies in the pure colloidal regime.

I. Introduction

THE colloid thruster is an electric propulsion concept characterized by the ejection of the propellant in the form of charged liquid droplets, accelerated by an electrostatic field. The liquid propellant is broken into droplets by an electrohydrodynamic process widely referred to as electrospray.[1–3] Electrosprays can atomize a liquid into fairly monodisperse drops, with a mean diameter controllable through the physical properties of the liquid and its flow rate. Drop diameters ranging from a few hundred microns down to some 20 nm have been reported. From the point of view of electrical propulsion, the usefulness of electrospray is rooted in its ability to generate highly charged droplets. The specific impulse associated with optimized propellants can exceed 500 s at high propulsion efficiency for acceleration voltages below 5 kV (Ref. 4). The use of electrohydrodynamic atomization by colloid thrusters is unique among other electric propulsion concepts. For example, ion and Hall thrusters ionize the propellant in the gas phase; magnetoplasma-dynamic thrusters ionize a fraction of the propellant in the gas phase, which is then accelerated along with neutrals; pulsed plasma thrusters typically ablate the propellant from a solid surface; and field emission electric propulsion generates ions by field evaporation from a liquid surface. Its charging process is responsible for the differentiating properties of colloid thrusters: the region in which charged drops form has submicron dimensions, making colloid thrusters suitable for micropropulsion. A wide range of flow rates can also be electrosprayed stably, enabling a substantial continuous variation of the thrust.

Research on the suitability of electrospray for space propulsion dates back to the early 1960s[5,6] and extended continuously into the following decade.[7] The colloid source most commonly used during that period consisted of multijet, highly stressed electrosprays of glycerol. Because of the relatively poor conductivity attainable (0.021 S/m for 19.3% weight of NaI in glycerol[8]), very high voltages were required to obtain colloid beams with reasonable specific impulses (values of 10 kV were typical). Even though successful prototypes were built,[9] interest in this technology decreased and eventually vanished. A more detailed account of this earlier era of colloid thrusters can be found in Ref. 10.

Interest in colloid thrusters has been reactivated in recent years,[4,11,12] mainly because of new types of space missions that need its peculiar propulsion characteristics. First, the expected proliferation of micro- and nanosatellites, made possible by advances in electronics and microfabrication techniques, is currently handicapped by the lack of efficient micropropulsion.[13] Second, there are several scientific and formation-flying missions in which the relative positions of spacecraft need to be controlled with great precision. For example, the Laser Interferometer Space Antenna, among other specifications, requires controlling spacecraft position within microns. Such requirements can be fulfilled via colloidal propulsion. In this context, the selection by NASA's New Millennium Program of the Disturbance Reduction System (DRS) as the Space Technology 7 (scheduled to fly by 2006, with a total budget of $62.6 million) represents a major boost for the development of colloid thruster technology.* The DRS is designed to validate system-level technology required for two types of future missions: measurements of planetary gravity and of cosmic gravitational waves and precision formation-flying interferometers.[14,15] The DRS is based on the concept of a freely floating test mass contained within a spacecraft that shields it from external forces. The test mass will ideally follow a trajectory determined only by the local gravitational field. The spacecraft position must be continuously adjusted to stay centered about the test mass, essentially flying in formation with it. An array of colloid thrusters will control the position of the spacecraft.

From the point of view of electrical propulsion, the key parameters one wishes to control to attain high performance are the distribution of charge-over-mass ratio $f(q/m)$ of the sprayed drops and the irreversible voltage drop ΔV associated with electrical inefficiency in the acceleration of the cone-jet.[4,8,16] ΔV appears to be generally small (∼200 V) compared to the acceleration voltage (∼2 kV). The mean q/m is of vital interest, because, at a given acceleration voltage, it controls the specific impulse. This quantity can be maximized by increasing the electrical conductivity of the propellant. The spread of q/m is also an important characteristic because exhaust beams with a wide specific charge distribution do penalize propulsion efficiency.[4] Fortunately, the distributions $f(q/m)$

Received 3 September 2002; revision received 19 December 2003; accepted for publication 19 December 2003.

*Graduate Student Assistant, Mechanical Engineering Department, 9 Hillhouse Avenue.
†Professor, Mechanical Engineering Department, 9 Hillhouse Avenue.
‡Research Scientist, 11 Tech Circle.

*Data available online at ftp://ftp.hq.nasa.gov/pub/pao/pressrel/2002/02-053.txt.

emerging from individual emitter tips are often relatively narrow, provided that certain necessary constraints are met. First, the Taylor cone formed at the electrified capillary tip must operate in the single cone-jet regime, where a steady axisymmetric jet is ejected from the cone apex.[2] Second, the breakup of this jet into drops must be regular, as is the case when the jet flow rate is not too far above the minimum value at which the cone-jet structure is stable and when a certain viscosity parameter governing the breakup of the jet into drops is adequately small.[17] These conditions are readily met with electrolytes of moderately viscous liquids. Finally, fuels must have a low volatility because the material lost by evaporation is not electrostatically accelerated and produces no thrust.

In conclusion, the ideal fuel for electrical propulsion must have low volatility and viscosity and high electrical conductivity. The best such propellant identified to date is formamide, with a room-temperature viscosity of 3.7 cP, and an ability to reach room-temperature electrical conductivities K above 2 S/m when seeded with inorganic salts. Although formamide's modest volatility allows production of stable Taylor cones in a vacuum, its finite evaporation rate demands that the meniscus be supported on relatively small tips, typically below 20 μm, but ideally at some 5 μm. This requirement is particularly important at the low propellant flow rates required to attain high specific impulses (see the following).

Formamide electrolyte drops can be made smaller and smaller (higher specific impulses) by adding more and more salt and by reducing liquid flow rate, but only to a point. Eventually, the electric field on the cone-tip region becomes large enough for ions to be field evaporated along with the drops.[18] The resulting mixed sprays are characterized by the appearance of two widely separated steps in the time-of-flight (TOF) spectra $I(t)$ resulting from interrupting the spray at time zero and recording the current I received by a collector as a function of subsequent time t. This behavior is illustrated in Fig. 1 for 16.8% (w) NaI in formamide, where the various curves included correspond to different liquid flow rates. The step arising at small flow rates at about $t = 1$ μs ($m/q \sim 0.003$ g/C) is associated with ions. The step to the right, whose position varies from 7 to 25 μs at increasing flow rates corresponds to droplets. The electrical propulsion characteristics of these sprays have been studied by Gamero-Castaño and Hruby.[4] In the mixed emission arising at small flow rates, where ions and drops form simultaneously, they find relatively poor associated propulsion efficiencies η_p, generally below 70%.

The purely ionic regime is easily attained in liquid metal ion sources and has been exploited for ion propulsion in so-called field emission electric propulsion.[19–21] Conditions approaching the pure ionic regime have been briefly mentioned for sulfuric acid,[22] but this notable observation has not been pursued further. Note in Fig. 1 that the ion current can be substantially larger than the drop's, apparently indicating that slight tuning changes could make the same thruster approach either an ion or a colloidal engine. Unfortunately, pure ion emission without accompanying drops has been so far elusive for electrolytes of organic solvents. Electrical conductivities in such electrolytes are in some cases high enough for the ions to dominate the current (Fig. 1). But the conductivities are insufficient for ionic emissions to dominate either the mass flow rate or the thrust. The appearance of ions therefore offers the possibility of increasing the specific impulse in formamide electrolytes, but only at the expense of considerable loss of propulsive efficiency.[4]

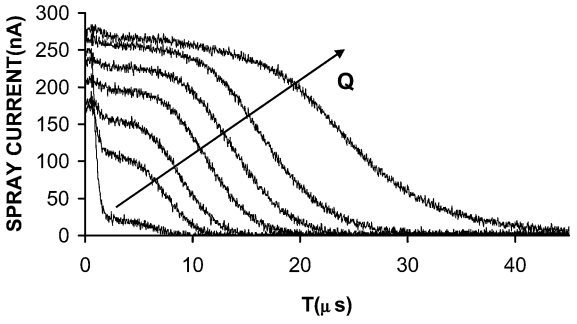

Fig. 1 TOF curves at different liquid flow rates Q for 16.8% (w) NaI in formamide. The steps arising at about $t = 1$ μs ($m/q \sim 0.003$ g/C) are caused by ions. Those to the right, whose position varies from 7–25 μs, are from drops.

The present study is part of a broad effort to increase the specific impulse attainable in colloidal thrusters, while avoiding the performance loss associated with the mixed ion-drop regime. One obvious strategy is to identify solvent-solute combinations where the ion evaporation regime is delayed, enabling the production of smaller drops (hence larger q/m) in the pure colloidal regime. Some background on the kinetics of ion evaporation from charged liquid surfaces will illuminate the search for an ideal ion-solvent pair. The mechanism and rate of ion evaporation from charged liquid surfaces has been the subject of considerable controversy following the first proposed model of Iribarne and Thomson.[23,24] However, their single-step activated mechanism has by now become fairly well established, and the rate of ionization can be safely taken to be proportional to

$$\text{ionization rate} \sim \exp\left\{\frac{-[\Delta G - \Delta(E, R)]}{kT}\right\} \tag{1}$$

where ΔG is the Gibbs free energy required for a solution ion to escape into the gas phase (generally in a solvated state). $\Delta G/kT$ is typically between 50 and 100, so that rates of ionization are negligible in the absence of intense electric fields. The term $\Delta(E, R)$ represents a reduction of the activation energy as a result of the large electric field E and small radius of curvature R of the emitting surface. But because this reduction is almost the same for all ions present in the solvent, the relative rates of evaporation of various ions are primarily determined by their corresponding ΔG values. Accordingly, ion evaporation is delayed in electrolytes where all cations in solution (or anions in negative electrosprays) have relatively large solvation energies. ΔG values have been reported for a variety of ions in water.[25] They vary slightly from 2.34 eV for Cs^+ to 2.495 for Li^+, with a trend that would lead one to expect even larger values for H^+. Data for NH_4^+ have been reported to be intermediate between Na^+ and K^+ (Ref. 25). However, based on the high level of protein charging observed in water ammonium acetate buffers,[26] we had reasons to suspect ΔG for NH_4^+ to be fairly high. Therefore, the proton and ammonium ions appeared as more promising than Na^+ for our purposes, at least from aqueous solutions. Water itself is an ideal solvent from the point of view of ion evaporation, with expected ΔG values considerably higher than for other organic solvents.[27] Unfortunately water is too volatile to be readily electrosprayable in a vacuum. Literature values for ΔG in nonaqueous solvents are even more scarce than for water, and the limited data available for formamide are for relatively large ions having undesirably small ΔG (Ref. 28). Given this lack of relevant information, we presently have no better choice than presuming the relative ΔG ordering of the diverse ions is similar in water and formamide. Because acids are generally undesirable in satellite plumes and some of the obvious acid candidates are reactive with formamide, the present study will be based on ammonium salts. We shall confirm that the ammonium ion is less volatile than Na^+.

II. Experimental

A. Vacuum Chamber

All experiments have been carried out in the vacuum chamber shown schematically in Fig. 2. It was evacuated by a small turbomolecular pump (Leybold, 50 lit/s) backed by a mechanical pump. The typical pressure level attained was several times 10^{-6} torr. The electrospray source is housed inside a four-arm cross (2-in. I.D.; left side of main chamber), connected to the wider and longer main chamber (6-in. I.D.) used for TOF measurements. The emitter and extractor electrodes are mounted coaxially in the branch of the cross opposite to the TOF chamber. The emitter is a 20-μm I.D. silica needle, whose outer diameter (360 μm) is sharpened into a conical tip to minimize the exposed area of the meniscus and hence the rate of solvent evaporation. The liquid to be electrosprayed is fed to this tip

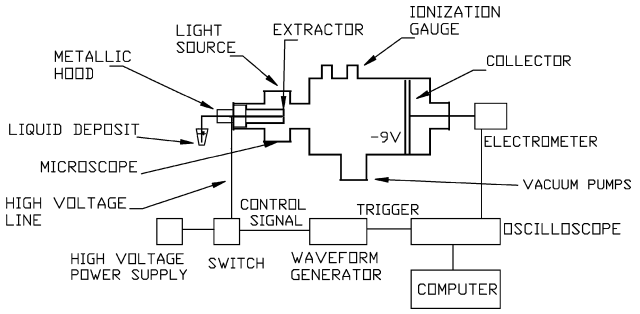

Fig. 2 Experimental setup.

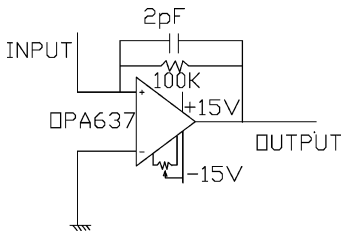

Fig. 3 Schematic of the electrometer.

through the silica needle from a polypropylene container (1 cm^3) located outside the vacuum. The liquid flow rate through the needle is controlled through the pressure inside the polypropylene container, which can be varied from 3 atm down to a fraction of one torr. The spraying end of the silica needle is supported inside a slightly wider centering metallic tube, which also provides the high-voltage contact to the meniscus. For this purpose, the tip region of the silica needle is coated with a conducting film of tin oxide. The extractor is a grounded cylinder (I.D. 9 mm), supported on the same flange as the needle, and coaxial with it. Its sides are provided with two openings, for visualization and illumination of the meniscus, both covered with fine wire mesh meant to avoid electromagnetic radiation to the collector from the switching high voltage needle. The end of this extractor tube facing the needle is closed with a metallic plate (thickness 0.8 mm) with a centered hole (diameter 2 mm; distance between needle tip and extractor orifice 2 mm). The dimensions of the vacuum chamber were designed so that a spray with a half angle of up to 25 deg would reach the collector without touching the walls of the chamber. The spray current is received inside the chamber by a collector (a metallic plate virtually grounded through an electrometer), preceded by a metallic mesh. This mesh is 90% transparent and biased to −9.5 V to reject secondary electrons formed by ion impingement on the collector. The distance between the mesh and the collector plate is 4 mm, and the flight distance L is 3.0 cm.

The *electrometer* is of the traditional inverting amplifier type shown in Fig. 3. The amplifier (OPA637BP; obtained from DigiKey) was specially selected for its speed. Because the voltage at the collector plate and the screen preceding it are both fixed, there is no charging current of this capacitive element, and the response time of the circuit is not deteriorated by use of a large collector. Most of our experiments have used a resistor R of 100 kΩ. The response time is determined by the product RC, where the capacitor introduced was of 2 pF (RC = 0.2 μs). This relatively fast response is demonstrated in Fig. 4, but comes at the price of a modest amplification (0.1 mV of response per nA of collected current), with a noise level of several nA. However, averaging of the waveform from 10 to 100 cycles (∼1 minute) gives adequate signal to noise.

Given the high sensitivity of this electrometer and the presence of intense radiation from the high-voltage switch, considerable care needs to be used in isolating the amplifier from external noise. In addition to using BNC cables for all electrometer connections, and carefully shielding all switching high-voltage lines (including the emitter needle, shielded by the extractor, and all metallic parts connected to the needle emerging outside the chamber), one needs to cover with a metallic mesh all of the holes made in the extractor to view the cone jet. In addition, it is important to introduce two

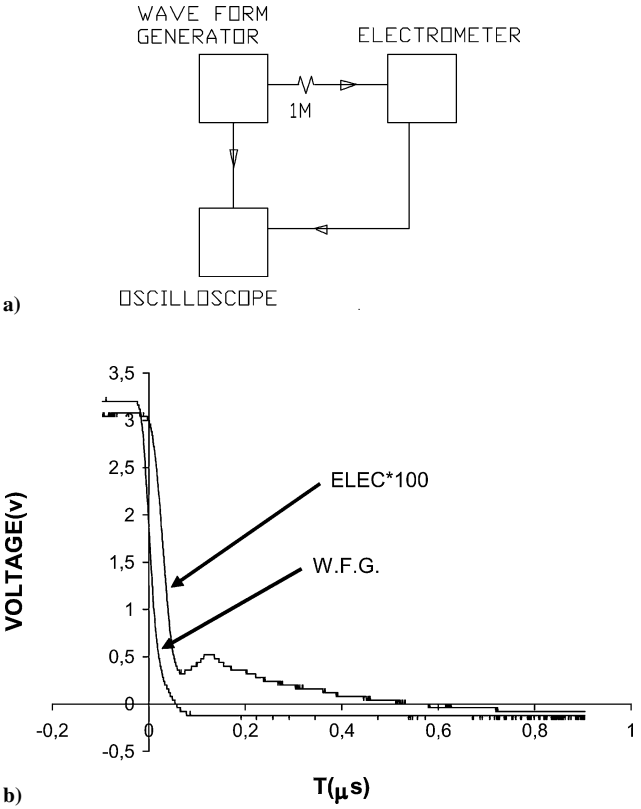

Fig. 4 Performance of the electrometer.

capacitors (100 pF) in the circuit between ground and the pair of ±15-V power inputs to the amplifier, to stabilize these voltages.

The *high-voltage switch* is used to periodically (∼1 Hz) interrupt the spray current, in order to measure the time-of-flight curves. The design used is almost identical to that of Ref. 4. A waveform generator (Fig. 2) produces a low-voltage signal controlling two high-voltage transistors, which ground the high-voltage output when the controlling value exceeds a threshold. The resistors in the switch were chosen to withstand a maximum voltage of 2 kV (CADDOCK Electronics, Inc. High performance film resistors). Each of the two transistors (IRFBG 30; DigiKey) is rated to 1 kV and controls half of the high voltage signal. The signal produced by the waveform generator is also used to trigger the digital oscilloscope (Tektronic TDS220) receiving the signal from the electrometer, which provides the origin of the TOF curves. These curves are transferred from the oscilloscope to a PC where they are stored.

B. Materials

Formamide and ammonium nitrate were from Sigma. Ammonium acetate was from Fluka. All salts used are hygroscopic and were dried for several hours under vacuum prior to weighing and mixing with the formamide. This precaution was not taken in prior work of Gamero-Castaño and Fernandez de la Mora,[18] where the water contained in the salt might have corrupted the inferred concentration. Water also reduces solution viscosity and tends to increase its electrical conductivity. In some cases, the use of hydrated salts also destabilizes the cone jet formed under vacuum. This might be caused by the rapid evaporation of the water component from the meniscus. Alternatively, loss of water would affect solubility, potentially giving raise to solute precipitation. Gamero and Hruby (private communication, 2001) have previously encountered difficulties in spraying solutions of undissecated ammonium acetate in a vacuum. No such problem was observed here with any of the dried salts.

III. Ammonium vs Sodium Electrolytes

Table 1 shows the characteristics of the various propellants used, all based on formamide. The data shown in Fig. 1 for NaI provide just a qualitative reference because part of the spray was intercepted

Table 1 Concentrations and conductivities (22°C) of the various formamide electrolytes used

Salt	Concentration (mole/lit of solvent)	Electrical conductivity, S/m
NH_4 acetate	1.76	1.01
NH_4 acetate	2.5	1.08
NH_4 acetate	3.0	1.09
NH_4 acetate	3.5	1.27
NH_4 acetate	4.0	1.13
NH_4 acetate	Saturated	0.96
NaI	16.8%w	1.49
NH_4NO_3	1.05	1.15
NH_4NO_3	2.1	1.68
NH_4NO_3	4.23	2.97

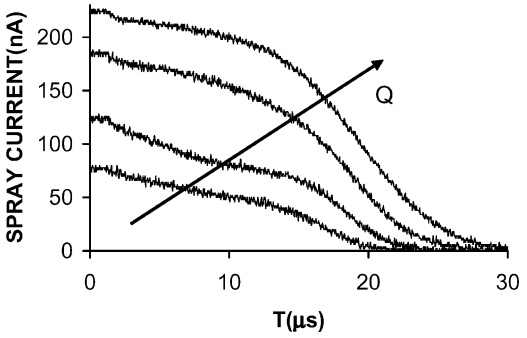

Fig. 5 TOF curves for formamide-ammonium acetate solutions (3 moles/liter of solvent) at various liquid flow rates Q.

by the extractor at the largest flow rates. This propellant has already been carefully studied,[4] and will not be investigated further here. TOF spectra for ammonium acetate (3 mol/lit of solvent) are shown in Fig. 5 at several liquid flow rates, labeled in the figure by the pressure (relative to atmospheric pressure) applied to the liquid reservoir. Table 2 collects the main parameters associated with these curves and all other similar curves studied. Except for the stopping voltage column (inferred from data such as those shown in Fig. 6, obtained similarly as in Ref. 4), all values in the table are moments of the time-of-flight distributions $I(t)$ measured (i.e., Figs. 1 and 5), where we use the same standard definitions of Gamero-Castaño and Hruby[4] for the mass flow rate m', the thrust T, and the propulsion efficiency η_p:

$$m' = \frac{4V_a}{L^2}\int_0^\infty I(t)t\,\mathrm{d}t \tag{2}$$

$$T = \frac{2V_a}{L}\int_0^\infty I(t)\,\mathrm{d}t \tag{3}$$

$$\eta_p = \frac{T^2}{2m'V_aI(0)} = \frac{\left\{\int_0^\infty I(t)\,\mathrm{d}t\right\}^2}{2I(0)\int_0^\infty I(t)t\,\mathrm{d}t} \tag{4}$$

Note that the mass flow rate m' does not account for any loss of fuel by evaporation from the meniscus, so that additional inefficiencies associated to evaporative losses are not accounted for in the tables. The number of decimals points included in the table are not fully warranted by the precision with which the $I(t)$ curves have been measured for many reasons, including our finite resolution in time and current, and the fact that the ion energy V_a has a finite distribution that has been ignored. Furthermore, our use of a flat collector in conjunction with a point source introduces an unaccounted factor of $1/\cos\theta$ in flight times for particles moving at polar angles θ with respect to the axis. Errors larger than several percent are therefore inevitable in most of the quantities reported in the table. The quantity $I(0)$ is the total spray current, which will be denoted as I. For the case where I is a step function centered at $t = t_0$, the propulsion efficiency reaches its maximum value of unity. Note

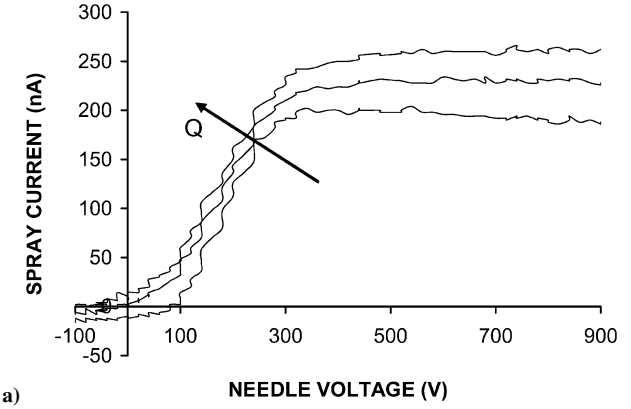

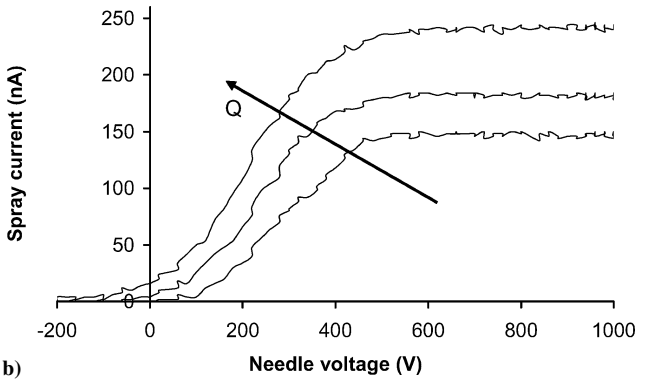

Fig. 6 Various examples of stopping potential curves for formamide-NaI solutions 16.6% (w) at different total emission current (asymptotic value of the current on the right), revealing that the mean irreversible voltage drop during cone-jet acceleration is about 200 V.

that this parameter does not incorporate the energy dissipation inefficiency associated to acceleration of the electrospray jet. These irreversibilities lead first to particle stopping voltages V_a smaller than the needle voltage V_n. As a result, the power consumption is not IV_a, but the larger quantity IV_n, which reduces the actual efficiency of the process. In addition, not all of the charged particles produced are necessarily ejected at the same voltage, which would modify the picture. Presumably, the dispersion in particle acceleration voltage further decreases the propulsive efficiency. In general, however, acceleration voltages differ from the needle voltage only in a few hundred volts, whereas needle voltages are in the range of several kilovolts. Hence this effect leads to manageable errors in the computation of propulsive parameters based on Eqs. (2–4). Most of these errors have in the past been accounted for by measuring the average acceleration voltage V_a for the whole spray by stopping potential (Fig. 6), and using it instead of V_n in Eqs.(2–4). In rigor, one should also modify the propulsion efficiency given in Eq. (4) by the additional inefficiency factor

$$\eta_{\mathrm{jet}} = V_a/V_n \tag{5}$$

though this is not systematically incorporated in all past work (i.e., Ref. 4). The separation between propulsion inefficiency caused by polydispersity in the q/m distribution [described by Eq. (4)] and the inefficency factor (5) is appropriate because the spray characteristics determining the jet loss $V_n - V_a$ and the polydispersity can be controlled independently of V_n (say by keeping the voltage difference between needle and extractor fixed, but further raising the needle voltage with respect to ground). At sufficiently large needle voltages the ratio (5) would approach unity, but the polydispersity parameter (4) would not change. Table 2 reports only the product $\eta_{\mathrm{jet}}\eta_p$, and should therefore not be compared directly with the η_p values of Ref. 4.

We stress the fact that the mass flow rate reported here is not measured directly from the liquid supply, but inferred from the TOF

Table 2 propulsion characteristics of the various fuels used

ΔP,[a] PSI	I,[b] nA	TOF, μs	V_n,[c] V	V_a,[d] V	m/q, g/C	m', kg/s	Thrust, μN	I_{sp},[e] s	$\eta_p\eta_{jet}$,[f] %	m'/I,[g] g/C
NH_4 acetate (1.76 moles per liter of solvent; K = 1.01 S/m)										
15	306	28	1500	1150	2.00	6.06E−10	6.17E−01	1.04E+02	68.46	1.98E+00
12.5	300	27.2	1500	1150	1.89	5.43E−10	5.75E−01	1.08E+02	67.73	1.81E+00
10	286	26	1500	1150	1.73	4.88E−10	5.36E−01	1.12E+02	68.69	1.71E+00
7.5	278	24	1500	1150	1.47	4.47E−10	5.04E−01	1.15E+02	68.28	1.61E+00
5	268	23.2	1500	1150	1.38	3.88E−10	4.56E−01	1.20E+02	66.74	1.45E+00
2.5	246	22	1500	1150	1.24	3.25E−10	4.01E−01	1.26E+02	66.90	1.32E+00
0	230	20.8	1500	1150	1.11	2.90E−10	3.68E−01	1.29E+02	67.47	1.26E+00
−1.23	218	19.8	1500	1150	1.00	2.42E−10	3.20E−01	1.35E+02	64.64	1.11E+00
−2.46	196	19	1500	1150	0.923	1.94E−10	2.70E−01	1.42E+02	63.81	9.89E−01
−3.68	182	18.2	1500	1150	0.846	1.71E−10	2.43E−01	1.45E+02	63.45	9.40E−01
−4.91	164	17.8	1500	1150	0.809	1.36E−10	2.02E−01	1.51E+02	60.74	8.29E−01
−6.14	148	17.4	1500	1150	0.773	1.13E−10	1.73E−01	1.56E+02	59.41	7.65E−01
−7.37	120	17	1500	1150	0.738	8.22E−11	1.33E−01	1.64E+02	59.45	6.85E−01
NH_4 acetate (2.5 moles per liter of solvent; K = 1.08 S/m)										
15	290	29.8	1500	1325	2.61	6.29E−10	6.47E−01	1.05E+02	76.60	2.17E+00
12.5	290	29	1500	1325	2.48	5.97E−10	6.32E−01	1.08E+02	76.98	2.06E+00
10	292	27.8	1500	1325	2.28	5.62E−10	6.11E−01	1.11E+02	75.93	1.92E+00
7.5	280	26.6	1500	1325	2.08	5.06E−10	5.74E−01	1.16E+02	77.45	1.81E+00
5	276	26	1500	1325	1.99	4.58E−10	5.37E−01	1.19E+02	76.01	1.66E+00
2.5	262	24.8	1500	1325	1.81	3.90E−10	4.83E−01	1.26E+02	76.12	1.49E+00
0	250	22.8	1500	1325	1.53	3.45E−10	4.43E−01	1.31E+02	75.77	1.38E+00
−1.23	236	22.2	1500	1325	1.45	2.96E−10	3.97E−01	1.37E+02	75.28	1.25E+00
−2.46	216	20.8	1500	1325	1.27	2.48E−10	3.49E−01	1.44E+02	75.92	1.15E+00
−3.68	210	19.8	1500	1325	1.15434	2.18E−10	3.18E−01	1.48E+02	73.44	1.04E+00
−4.91	182	19.4	1500	1325	1.108171	1.72E−10	2.66E−01	1.57E+02	75.09	9.47E−01
−6.14	166	18.4	1500	1325	0.996871	1.38E−10	2.24E−01	1.65E+02	72.88	8.31E−01
−7.37	150	17.8	1500	1325	0.932918	1.03E−10	1.76E−01	1.74E+02	66.80	6.88E−01
NH_4 acetate (3 moles per liter of solvent; K = 1.09 S/m)										
15	230	19.4	1552	1327	1.109844	2.37E−10	3.56E−01	1.53E+02	74.62	1.03E+00
12.5	222	18.8	1552	1327	1.042255	2.16E−10	3.31E−01	1.56E+02	73.53	9.74E−01
10	210	18.2	1552	1327	0.97679	1.93E−10	3.03E−01	1.60E+02	73.19	9.17E−01
7.5	192	17.4	1552	1327	0.892806	1.61E−10	2.63E−01	1.66E+02	71.95	8.38E−01
5	176	17.2	1552	1327	0.872399	1.34E−10	2.26E−01	1.71E+02	69.58	7.64E−01
2.5	150	17	1552	1327	0.852229	1.03E−10	1.79E−01	1.78E+02	67.03	6.84E−01
0	128	16.8	1552	1327	0.832294	8.05E−11	1.45E−01	1.83E+02	65.41	6.29E−01
−1.23	100	16.6	1552	1327	0.812596	5.91E−11	1.07E−01	1.85E+02	62.64	5.91E−01
−2.46	84	16.2	1552	1327	0.773906	4.22E−11	8.38E−02	2.02E+02	63.75	5.02E−01
NH_4NO_3 (1.05 moles per liter of solvent; K = 1.15 S/m)										
0	306	19.6	1595	1320	1.1269	3.69E−10	5.27E−01	1.46E+02	77.18	1.21E+00
−1.23	282	18.8	1595	1320	1.037	3.16E−10	4.70E−01	1.52E+02	77.78	1.12E+00
−2.46	274	17.6	1595	1320	0.909	2.71E−10	4.28E−01	1.61E+02	77.47	9.88E−01
−3.68	264	17	1595	1320	0.848	2.46E−10	3.97E−01	1.65E+02	76.05	9.31E−01
−4.91	228	15.2	1595	1320	0.678	1.86E−10	3.22E−01	1.76E+02	76.74	8.17E−01
−6.14	210	14.6	1595	1320	0.625	1.61E−10	2.86E−01	1.81E+02	75.79	7.66E−01
−7.37	194	13.6	1595	1320	0.542	1.32E−10	2.48E−01	1.91E+02	75.07	6.83E−01
−8.59	184	12.8	1595	1320	0.480	1.06E−10	2.12E−01	2.04E+02	72.35	5.76E−01
−9.82	142	11.6	1595	1320	0.394	6.41E−11	1.42E−01	2.25E+02	69.11	4.52E−01
NH_4NO_3 (2.11 moles per liter of solvent; K = 1.68 S/m)										
0	362	16.4	1592	1317	0.789	3.22E−10	5.21E−01	1.65E+02	73.07	8.90E−01
−1.23	354	15.6	1592	1317	0.714	2.97E−10	5.00E−01	1.72E+02	74.64	8.39E−01
−2.46	324	14.4	1592	1317	0.608	2.38E−10	4.27E−01	1.83E+02	74.14	7.35E−01
−3.68	332	13.2	1592	1317	0.511	2.28E−10	4.25E−01	1.90E+02	74.90	6.87E−01
−4.91	324	12.4	1592	1317	0.451	2.00E−10	3.92E−01	2.00E+02	74.80	6.16E−01
−6.14	302	12	1592	1317	0.422	1.64E−10	3.43E−01	2.13E+02	74.76	5.43E−01
−7.37	272	11.6	1592	1317	0.395	1.27E−10	2.87E−01	2.30E+02	74.84	4.66E−01
−8.59	248	9.8	1592	1317	0.282	9.55E−11	2.37E−01	2.53E+02	74.30	3.85E−01
−9.82	216	9.2	1592	1317	0.248	5.58E−11	1.66E−01	3.03E+02	71.64	2.58E−01

(Continued)

curves. Hence the mass flow rate reported represents the actual mass of charged material ejected from the Taylor cone tip and does not include neutrals lost by evaporation. The electrical conductivities reported are for the bulk liquid. Evaporation of the salt or the solvent could lead to a different local conductivity at the emitting tip of the Taylor cone.

Several important differences between Fig. 1 (for NaI) and 5 (for ammonium acetate) must be noted. First, although electrical conductivities differ by less than 40%, there are far larger differences in the minimum flow rates at which the spray is stable (4.2×10^{-11} Kg/s for NH_4^+ vs 3.52×10^{-12} Kg/s for Na^+), as well as in the corresponding times of flight for the respective drops (7 vs 15 μs, implying a four-fold increase in the m/q ratio from sodium to ammonium electrolytes). These differences preclude a clear conclusion on whether or not ammonium salts delay ion evaporation. For instance, there is almost no ion evaporation from either the ammonium electrolytes or the sodium solutions whose drops have comparable or larger $m/q(t > 17\ \mu s)$. On the other hand, for a given solvent and electrical conductivity, and in the absence of ion evaporation, drop m/z is known to be essentially independent of the specific anion and

Table 2 propulsion characteristics of the various fuels used (continued)

ΔP,[a] PSI	I,[b] nA	TOF, μs	V_n,[c] V	V_a,[d] V	m/q, g/C	m', kg/s	Thrust, μN	I_{sp},[e] s	$\eta_p\eta_{jet}$,[f] %	m'/I,[g] g/C
NH_4NO_3 (4.23 moles per liter of solvent; K = 2.97 S/m)										
−7.37	270	——	1600	——	0.30	7.80E−11	0.229	299	77.80	0.29
−8.59	212	——	1600	——	0.25	5.58E−11	0.173	317	79.43	0.26
−9.82	120	——	1600	——	0.16	2.34E−11	0.086	374	81.94	0.19
INa (16.8% by weight; K = 1.49 S/m)										
15	290	27.00	1515	1350	2.187	5.26E−10	5.89E−01	1.14E+02	75.04	1.81E+00
12.5	288	26.40	1515	1350	2.09	5.03E−10	5.80E−01	1.17E+02	76.51	1.75E+00
10	294	25.00	1515	1350	1.87	4.66E−10	5.60E−01	1.23E+02	75.67	1.58E+00
7.5	292	23.80	1515	1350	1.70	4.26E−10	5.38E−01	1.29E+02	76.88	1.46E+00
5	296	22.80	1515	1350	1.56	3.95E−10	5.19E−01	1.34E+02	76.15	1.33E+00
2.5	294	22.20	1515	1350	1.48	3.56E−10	4.92E−01	1.41E+02	76.30	1.21E+00
0	284	21.00	1515	1350	1.32	3.21E−10	4.64E−01	1.48E+02	78.13	1.13E+00
−1.23	274	19.40	1515	1350	1.13	2.78E−10	4.28E−01	1.57E+02	79.47	1.01E+00
−2.46	274	17.60	1515	1350	0.929	2.42E−10	3.94E−01	1.66E+02	77.08	8.85E−01
−3.68	266	16.40	1515	1350	0.807	2.15E−10	3.66E−01	1.74E+02	77.39	8.08E−01
−4.91	250	15.40	1515	1350	0.711	1.77E−10	3.26E−01	1.87E+02	79.16	7.09E−01
−6.14	238	13.40	1515	1350	0.539	1.47E−10	2.90E−01	2.01E+02	79.32	6.16E−01
−7.37	236	12.00	1515	1350	0.432	1.17E−10	2.51E−01	2.19E+02	75.57	4.94E−01
−8.59	220	9.80	1515	1350	0.288	8.62E−11	2.07E−01	2.45E+02	74.84	3.92E−01
−9.82	196	9.40	1515	1350	0.265	5.26E−11	1.53E−01	2.96E+02	74.51	2.69E−01
−10.31	194	8.20	1515	1350	0.202	3.93E−11	1.26E−01	3.27E+02	68.97	2.03E−01
−10.8	192	7.60	1515	1350	0.173	4.11E−11	1.29E−01	3.21E+02	69.90	2.14E−01
−11.29	182	6.60	1515	1350	0.131	2.88E−11	1.02E−01	3.62E+02	65.71	1.58E−01
−11.78	186	6.00	1515	1350	0.108	2.00E−11	8.07E−02	4.10E+02	57.65	1.08E−01
−12.03	208	5.60	1515	1350	0.0941	1.14E−11	5.71E−02	5.10E+02	45.32	5.49E−02
−12.27	254	5.40	1515	1350	0.0875	6.34E−12	4.40E−02	7.07E+02	39.68	2.50E−02
−12.52	252	5.00	1515	1350	0.075	3.52E−12	3.39E−02	9.81E+02	42.72	1.40E−02

[a] ΔP = pressure (relative to the atmosphere) in the liquid supply chamber.
[b] I = total spray current.
[c] V_n = needle voltage.
[d] V_a = acceleration voltage (from stopping voltage measurement).
[e] I_{sp} = specific impulse = thrust/(g m′) and $g = 9.8$ m/s^2.
[f] η_p and η_{jet} are defined in Eqs. (4) and (5).
[g] Note that m' does not take into account evaporative losses of liquid from the meniscus.

cation in the salt. Accordingly, the large differences observed in m/q for both solutions at comparable flow rates and bulk conductivities imply that the local electrical conductivities at the apex of the two Taylor cone jets must be quite different from each other. This observation betrays large effects associated with liquid and solute evaporation. Indeed, Gamero-Castaño and Hruby[4] have measured about 50% evaporative loss of solvent in Taylor cones of formamide-NaI at the smallest flow rates and largest electrical conductivities tried. For the case of an involatile salt, such as NaI, this implies a doubling of the average salt concentration in the tip region. The local salt concentration on the surface region (where the solvent evaporates) must be considerably more than doubled, leading inevitably to greatly enhanced local electrical conductivities. The opposite effect would arise for a solute such as ammonium acetate, which is more volatile than the solvent (as evident from the fact that salt precipitation was never observed from formamide-ammonium acetate solution drops evaporating under vacuum). The net result would be a considerably larger surface tip conductivity for the sodium than for the ammonium salts, which would rationalize the large differences observed in the corresponding electrosprays.

We anticipate that the practical problems and ambiguities created by the evaporation of formamide will eventually be resolved by miniaturization of the emitters. Indeed, the future of colloidal propulsion will necessarily be based on large arrays of micromachined emitters, because single emitters produce exceedingly small (sub-μN) thrusts. Use of individual Taylor cones with tip dimensions of about one or a few microns is relatively common in so called nanospray mass spectrometry.[29,30] Similar miniaturized sources would reduce the evaporative loss by a factor of 400, making it essentially negligible for formamide.

Although new microsources are being developed, we have investigated the involatile salt NH_4NO_3, (a strong oxidant), whose formamide electrolytes ought to behave similarly to those of NaI in all respects, except for the different ionic volatilities of the respective

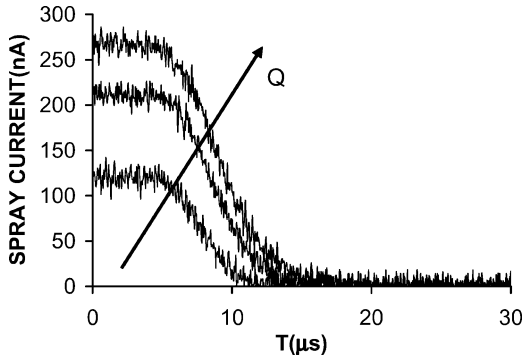

Fig. 7 TOF curves for formamide-NH_4NO_3 (4.23 mole/lit of solvent) at various flow rates Q. The flight times for the drops are comparable to those in Fig. 1 for NaI, but ion evaporation has now been suppressed. The lack of ion evaporation also keeps drop currents far above those in Fig. 1. As a result, at comparable m/q values for the drops the nitrate solutions produce more than twice the thrust at almost twice the efficiency $\eta_p\eta_{jet}$ (82% vs 43%).

cations. Both solutions would lose formamide and become similarly enriched in their respective salts. Figure 7 shows TOF curves for NH_4NO_3 in formamide (4.23 mole/lit of solvent). Note now that the smallest flow rates reached lead to comparable flight times for the drops in the nitrate and the iodide solutions. This implies that the two local electrical conductivities at the cone tip are comparable. On the other hand, ion evaporation is entirely absent from the nitrate solutions, yet dominates the current in the NaI solutions. As a result, at comparable m/q values for the drops the nitrate solutions produce considerably more thrust at a substantially higher propulsive efficiency ($\eta_p\eta_{jet} = 82\%$ vs 65% at $I_{sp} \sim 374$ s). This point can be seen in Fig. 8, which shows specific impulse as a function of thrust for all of the data in Table 2. At a given specific impulse,

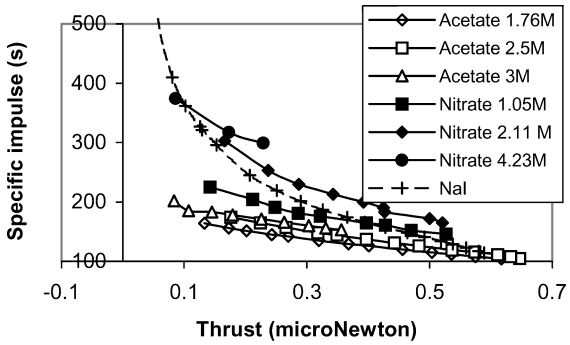

Fig. 8 Specific impulse as a function of thrust for all of the data in Table 2. The nitrate data outperform all others at thrusts larger than 0.1 μN not only in thrust level at given specific impulse, but also in propulsion efficiency. At thrust below 0.1 μN, NaI electrolytes yield a better specific impulse than nitrate electrolytes, though still at a lower propulsion efficiency.

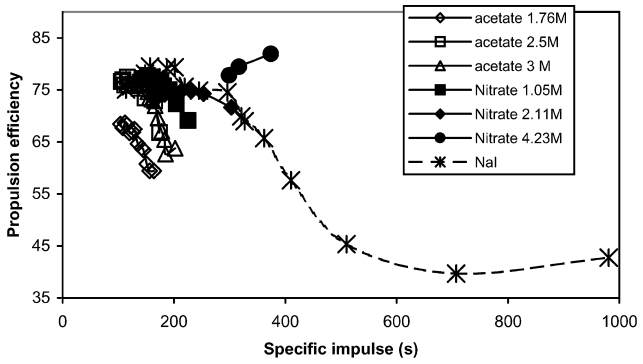

Fig. 9 Propulsion efficiency plotted as a function of specific impulse. Note the considerable advantage of the ammonium nitrate solutions at specific impulses above 300 s.

the nitrate yields more thrust per Taylor cone at specific impulses below 370 s. Interestingly, above I_{sp} 370 s, NaI electrolytes offer more thrust than nitrate electrolytes, though still at a lower propulsion efficiency. This advantage in net thrust follows from the rapid increase in the current level associated to the onset of the ionization regime. The superior performance of the involatile nitrate vs the volatile acetate is striking under all conditions.

The propulsion efficiency is represented in Fig. 9 as a function of specific impulse, showing a poorer performance of the volatile salts with respect to the nitrates and the NaI. The sharp loss of efficiency of the ammonium acetate solutions with increased specific impulse is to be expected from the fact that higher I_{sp} requires smaller flow rate, and this leads to larger transit time of the solution in the Taylor cone and more evaporative loss of solvent. The NaI and nitrate salts are quite comparable below $I_{sp} = 300$ s. Above this value the efficiency for NaI solutions begins to drop precipitously because of ion evaporation, whereas that of the nitrate actually increases.

In conclusion, the volatile salt has undesirable characteristics from all viewpoints other than the avoidance of salt precipitation and needle clogging. Ammonium nitrate is comparable to NaI, except at the high conductivities where ion evaporation sets in for Na^+ but not for NH_4^+. The advantage of ion evaporation suppression manifests itself not only in a higher propulsion efficiency, but also in a higher thrust level per Taylor cone at fixed I_{sp}. The thrust advantage is eventually lost when ions begin to dominate the emission of the NaI solutions and net currents rise above the pure drop regime level. The efficiency advantage of the ammonium nitrate solution remains over the whole range of conditions explored, but would eventually disappear if a purely ionic regime were to be attained. In practice we have not been able to extend the purely colloidal regime of ammonium nitrate beyond $I_{sp} > 370$ s due to solvent evaporation and salt precipitation. But there is no fundamental reason why this range could not be extended further in other solvent solute combinations, or in this same system with a smaller capillary tip leading to reduced evaporative losses.

We note finally that the propulsive efficiencies reported can be increased by accelerating further the particles following the extractor electrode. This postacceleration would affect neither the current nor the irreversible voltage drop, but it would increase the factor (5). Hence, postacceleration to 5 kV would yield $\eta_{\text{jet}}\eta_p > 90\%$ in almost all tests with ammonium nitrate. The corresponding specific impulse would increase from the 374 s reported in Table 2 to 728 s. The performance obtained with this propellant is by far the best so far reported for colloidal devices. However, operating at 4.23 moles per liter of solvent is rather difficult because of the tendency of the ammonium nitrate to precipitate when the meniscus is subject to a vacuum. It would be impractical to use such a fuel in a satellite thruster, unless the rate of solvent evaporation is drastically reduced by miniaturization or alternative means.

Notice a most interesting difference in the minimum flow rates reached, 3.52×10^{-12} Kg/s for Na^+, vs 23.4×10^{-12} Kg/s for NH_4^+. Because the mass flow rate over current ratio for the drops is equal to their associated m/q, which is similar in both cases, the large observed mismatch in flow rates must necessarily be accompanied by a large mismatch in currents. Indeed, the drop current is of $\sim$20 nA (sodium) vs 120 nA (ammonium). In other words, the onset of the ion evaporation regime seems to trigger a drastic reduction in the emitted drop current at a given drop mass to charge ratio. This large departure from the ordinary trend of the pure drop regime of electrosprays could potentially lead to the existence of a purely ionic regime. Put another way, in the pure drop regime it is impossible to eject a steady current without pushing a relatively large flow through the jet. If the relation between drop current and liquid flow rate characteristic of the pure drop regime remained unchanged in the presence of ion evaporation, it would still be impossible to emit mostly ions. What our experiments show is that the usual pure drop trend changes drastically following the onset of ion evaporation, leading to a large reduction in the mass flow rate necessary to maintain a stable cone jet. If the observed trend (larger increases in ionic currents enable continuous reductions in the drop current) were to continue at higher electrical conductivities, it might be possible to reach a purely ionic electrospray regime with no drop production, as in the case of liquid metals.

IV. Conclusions

Comparison of the propulsion characteristics of formamide solutions seeded with either sodium or ammonium salts leads to the following conclusions:

1) The high solvation energy of the ammonium ion virtually eliminates ion evaporation from electrolytes of formamide with ammonium salts and permits reaching a specific impulse as lare as 370 s with relatively high propulsion efficiencies.

2) The nonnegligible volatility of formamide needs to be compensated by use of capillary tip diameters considerably smaller than the 20 μm used here.

3) Use of formamide seeded with volatile ammonium salts eliminates clogging problems associated with salt precipitation at the emitter tip. However, evaporative loss of the salt leads to poor performance. If this problem is eliminated with micromachined emitters , this fuel could provide an excellent fuel for electrical propulsion.

4) Comparison of ion-emitting (NaI) with non-ion-emitting (NH_4NO_3) shows that the onset of ion evaporation not only decreases propulsion efficiency, but also lowers the thrust attainable by rapidly reducing drop current. Although undesirable from the viewpoint of colloidal propulsion, this finding might indicate the viability of purely ionic propulsion from Taylor cones of slightly more conducting solutions or more volatile ions.

Acknowledgment

This study has been supported initially by Busek Co., Inc. [subcontract from a a NASA small business innovative research (SBIR) program] and subsequently by U.S. Air Force office of Scientific Research Grant F-49620-01-1-0416. We are much indebted to our

colleagues at Sciex for their gift of a turbopump. The inputs from V. Hruby (Busek), M. Martinez-Sanchez Massachusetts Institute of Technology, Ismael Guerrero and Ignacio Romero (both from Yale) are gratefully acknowledged.

References

[1]Fenn, J. B., Mann, M., Meng, C. K., Wong, S. F., and Whitehouse, C., "Electrospray Ionization for Mass Spectrometry of Large Biomolecules," *Science*, Vol. 246, No. 4926, 6 Oct. 1989, pp. 64–71.

[2]Cloupeau, M., and Prunet-Foch, B., "Electrostatic Spraying of Liquids: Main Functioning Mode," *Journal of Electrostatics*, Vol. 25, No. 2, Oct. 1990, pp. 165–184.

[3]Fernández de la Mora, J., and Loscertales, I. G., "The Current Emitted by Highly Conducting Taylor Cones," *Journal Fluid Mechanics*, Vol. 260, 1994, pp. 155–184.

[4]Gamero-Castaño, M., and Hruby, V., "Electrospray as a Source of Nanoparticles for Efficient Colloid Thrusters," *Journal of Propulsion and Power*, Vol. 17, No. 5, 2001, pp. 977–987.

[5]Krohn, V. E., "Liquid Metal Droplets for Heavy Particle Propulsion," *Progress in Astronautics and Rocketry*, Vol. 5, edited by David B. Langmuir, Ernst Stuhlinger, and J. M. Sellen, Jr., A. C. Press, New York, 1961, pp. 73–80.

[6]Krohn, V. E., "Glycerol Droplets for Electrostatic Propulsion," American Rocket Society Electric Propulsion Conference, Berkeley, CA, 1962.

[7]Huberman, M. N., and Rosen, S. G., "Advanced High-Thrust Colloid Sources," *Journal of Spacecraft and Rockets*, Vol. 11, No. 7, 1974, pp. 475–480.

[8]Huberman, M. N., "Measurement of the Energy Dissipated in the Electrostatic Spraying Process," *Journal of Applied Physics*, Vol. 41, No. 2, 1970, pp. 578–584.

[9]Kidd, P. W., and Shelton, H., "Life Test (4350 hrs.) of an Advanced Colloid Thruster Module," AIAA Paper 73-1077, 1973.

[10]Martinez-Sánchez, M., Fernández de la Mora, J., Hruby, V., Gamero-Castaño, M., and Khayms, V., "Research on Colloid Thrusters," *Proceedings of the 26th International Electric Propulsion Conference*, Kitakyushu, Japan, Oct. 1999.

[11]Gamero-Castaño, M., and Hruby, V., "Characterization of a Colloid Thruster Performing in the Micro-Newton Thrust Range," 27th International Electric Propulsion Conference, IEPC Paper 01-282, Oct. 2001.

[12]Pranajaya, A., and Capelli, M., "Performance Studies of a Colloid Thruster System," International Electric Propulsion Conference, Paper 01-284, Oct. 2001.

[13]Mueller, J., "Thruster Options for Microspacecraft: A Review and Evaluation of Existing Hardware and Emerging Technologies," AIAA Paper 97-3058, July 1997.

[14]Folkner, W. M., Buchman, S., Byer, R. L., DeBra, D., Dennehy, C. J., Gamero-Castaño, M., Hanson, J., Hruby, V., Keiser, G. M., Kuhnert, A., Markley, F. L., Houghton, M., Maghami, P., Miller, D., Prakash, S., and Spero, R., "Disturbance Reduction System: Testing Technology for Precision Formation Control," *Proceeding of Society of Photo-Optical Instrumentation Engineers*, Vol. 4860, The International Society for Optical Engineering, Waikoloa, HI, Aug. 2002, pp. 221–228.

[15]Hanson, J., Keiser, G. M., Buchman, S., Byer, R. L., Folkner,W. M., Hruby, V., and Gamero-Castaño, M., "Disturbance Reduction System for Testing Technology for Drag-Free Operation," *Proceeding of Society of Photo-Optical Instrumentation Engineers*, Vol. 4856, The International Society for Optical Engineering, Waikoloa, HI, Aug. 2002, pp. 9–18.

[16]Gamero-Castaño, M., and Hruby, V., "Electric Measurements of Charged Sprays Emitted by Cone-Jets," *Journal of Fluid Mechanics*, Vol. 459, May 2002, pp. 245–276.

[17]Rosell-Llompart, J., and Fernández de la Mora, J., "Generation of Monodisperse Droplets 0.3 to 4 mm in Diameter from Electrified Cone-Jets of Highly Conducting and Viscous Liquids," *Journal of Aerosol Science*, Vol. 25, No. 6, Sept. 1994, pp. 1093–1119.

[18]Gamero-Castaño, M., and Fernández de la Mora, J., "Direct Measurement of Ion Evaporation Kinetics from Electrified Liquid Surfaces," *Journal of Chemical Physics*, Vol. 113, No. 2, July 2000, pp. 815–832.

[19]Tajmar, M., and Wang, J., "Three-Dimensional Numerical Simulation of Field-Emission-Electric-Propulsion Neutralization," *Journal of Propulsion and Power*, Vol. 16, No. 3, 2000, pp. 536–544.

[20]Nobili, A. M., Bramanti, D., Polacco, E., Catastini, G., Anselmi, A., Portigliotti, S., Lenti, A., and Severi, A., "The Galileo Galilei (GG) Project: Testing the Equivalence Principle in Space and on Earth," *Advances in Space Research*, Vol. 25, No. 6, 2000, pp. 1231–1235.

[21]Marcuccio S., Genovese A., and Andrenucci M., "Experimental Performance of Field Emission Microthrusters," *Journal of Propulsion and Power*, Vol. 14, No. 5, 1998, pp. 774–781.

[22]Perel, J., Mahoney, J. F., Moore, R. D., and Yahiku, A. Y., "Research and Development of a Charged-Particle Bipolar Thruster," *AIAA Journal*, Vol. 7, No. 3, 1969, pp. 507–511.

[23]Iribarne, J. V., and Thomson, B. A., "On the Evaporation of Small Ions from Charged Droplets," *Journal of Chemical Physics*, Vol. 64, No. 6, 1976, pp. 2287–2294.

[24]Thomson, B. A., and Iribarne, J. V., "Field Induced Ion Evaporation from Liquid Surfaces at Atmospheric Pressure," *Journal of Chemical Physics*, Vol. 71, No. 11, 1979, pp. 4451–4463.

[25]Tang, L., and Kebarle, P., "Dependence of Ion Intensity in Electrospray Mass Spectrometry on the Concentration of the Analyte in the Electrospray Solution," *Analytical Chemistry*, Vol. 65, No. 24, 1993, pp. 3654–3688 (see Table II).

[26]Fernandez de la Mora, J., "Electrospray Ionization of Large Multiply Charged Species Proceeds via Dole's Charged Residue Mechanism," *Analytica Chimica Acta*, Vol. 406, No. 1, 1 Feb. 2000, pp. 93–104.

[27]Labowsky, M., Fenn, J. B., and Fernandez de la Mora, J., "A Continuum Model for Ion Evaporation from a Drop: Effect of Curvature and Charge on Ion Solvation Energy," *Analytica Chimica Acta*, Vol. 406, No. 1, 1 Feb. 2000, pp. 105–118.

[28]Loscertales, I. G., and Fernández de la Mora, J., "Experiments on the Kinetics of Field-Evaporation of Small Ions from Droplets," *Journal of Chemical Physics*, Vol. 103, No. 12, Sept. 1995, pp. 5041–5060.

[29]Wilm, M. S., and Mann, M., "Analytical Properties of the Nanoelectrospray Ion Source," *Analytical Chemistry*, Vol. 68, No. 1, 1996, pp. 1–8.

[30]Dohmeier, D. M., and Jorgenson, J. W., "Microelectrospray Method and Apparatus," U.S. Patent 5,115,131, 1992.